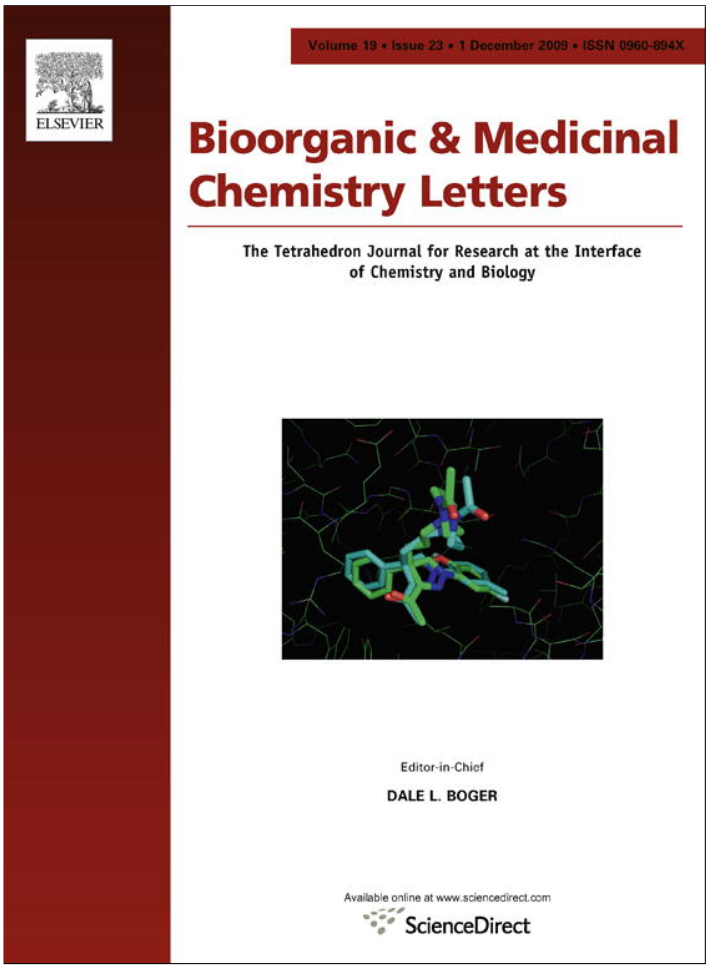

Bioorganic & Medicinal Chemistry Letters 19 (2009) 6709–6712

Contents lists available at ScienceDirect

Bioorganic & Medicinal Chemistry Letters

journal homepage: www.elsevier.com/locate/bmcl

# A plausible role of salivary copper in antimicrobial activity of histatin-5—Metal binding and oxidative activity of its copper complex

William M. Tay [a], Ahmed I. Hanafy [b], Alexander Angerhofer [c], Li-June Ming [a,*]

[a] Department of Chemistry and MBIG, University of South Florida, Tampa, FL 33620-5250, USA
[b] Department of Chemistry, Faculty of Science, Al-Azhar University, Nasr City, Cairo, Egypt
[c] Department of Chemistry, University of Florida, Gainesville, FL 32611, USA

ARTICLE INFO

*Article history:*
Received 5 July 2009
Revised 26 September 2009
Accepted 30 September 2009
Available online 3 October 2009

*Keywords:*
Antibiotic
Cobalt
Copper
Catechol
EPR
Histatin
Metallopeptide
NMR
Oxidation

ABSTRACT

Histatin-5 (Hn5) is an antimicrobial salivary peptide of 24 amino acids. Two specific metal-binding sites were revealed with electronic, NMR, and EPR spectroscopy. The complex $Cu_2^{II}$–Hn5 effectively oxidizes catechol, exhibiting enzyme-like kinetics ($k_{cat} = 0.011$ and $0.060\ s^{-1}$ and $k_{cat}/K_m = 19$ and $50\ M^{-1}\ s^{-1}$ without and with 12.8 mM $H_2O_2$, respectively). The significant oxidative activity may contribute to the biological activity of this antibiotic metallopeptide.



The histatins (Hns) are antimicrobial cationic peptides, secreted by parotid and submandibular glands,[1] exhibiting activities against *Streptococcus mutans*, *Streptococcus mitis*, *Saccharomyces cerevisiae*, *Cryptococcus neoformans*, and *Porfiromonas gengivalis*.[2–5] They are also fungistatic and fungicidal against the prevalent and opportunistic pathogenic yeast *Candida albicans*,[6] inhibit experimental plaque formation and gingivitis,[7] and are suggested to be major wound-closure stimulating factors in human saliva.[8] Hns are mainly expressed as Hn1 and Hn3 in higher primates,[9,10] of which Hn5 is the most abundant in the saliva. It consists of the first 24 amino acids (DSHAK RHHGY KRKFH EKHHS HRGY) of Hn3 and displays the highest activity against *C. albicans* under physiological concentrations (15–30 μM).[1] Unlike many other antibiotic peptides, Hn5 cannot form pores in the bacterial cell membranes.[11] One antifungal mechanism suggests internalization of Hn5 by binding to the heat shock protein Ssa1/2 on the cell wall,[12] followed by interaction with the $K^+$ transporter TRK1[13] which leads to the release of $K^+$, ATP, and other cell components and subsequently results in apoptosis.[14] Alternatively, Hn5 is internalized into the mitochondria and interferes with the electron transfer processes, which leads to the generation of reactive oxygen species and oxidative damage.[15] Moreover, synthetic variants of Hn5 exhibit oxidative nuclease activity in the presence of $Cu^{II}$, suggesting a possible role of metal ions in the action of Hns.[16]

Hn3 and Hn5 have previously been suggested to bind up to 5 equiv of different metal ions, including $Cu^{II}$, $Ni^{II}$, $Zn^{II}$, $Fe^{II}$, and $Ca^{II}$,[17] and can fuse negatively charged vesicles in the presence of $Zn^{II}$.[17a] Hn5 has a high-affinity $Cu^{II}$ and $Ni^{II}$ binding site at the N-terminus (analogous to the N-terminal metal-binding ATCUN site of Asp-Ala-His in serum albumin[18]) and a presumed $Zn^{II}$ binding site (HEXXH). Herein, we report metal binding of Hn5 and a unique oxidative activity of its $Cu^{II}$ complex by means of magnetic resonance and kinetic methods.

Upon addition of 0.5-equiv $Cu^{II}$ to Hn5 in buffer at pH 7.0, an absorption at 520 nm is detected (Fig. 1). This absorption has a higher energy than that of a regular tetragonally distorted octahedral $Cu^{II}$ center, characteristic of the d–d transition in a square planar $Cu^{II}$ geometry attributable to $Cu^{II}$ binding to the N-terminus of Hn5 (Asp-Ser-His). It also corroborates with the $Cu^{II}$ in the N-terminal ATCUN site (Asp-Ala-His) of serum albumin at 525 nm[18,19] and the N-terminal fragment of Hn5.[16a] A plot of the absorption at 525 nm versus [$Cu^{II}$] yields a dissociation constant of 0.27 mM for $Cu^{II}$ binding to the N-terminus (inset, Fig. 1). Absorptions at 250, 300, and 620 nm become visible with more $Cu^{II}$ added and become distinct at >2.0-equiv $Cu^{II}$. The 620-nm absorption may be

* Corresponding author. Tel.: +1 813 974 2220; fax: +1 813 974 3203.
*E-mail address:* ming@shell.cas.usf.edu (L.-J. Ming).

0960-894X/$ - see front matter © 2009 Elsevier Ltd. All rights reserved.
doi:10.1016/j.bmcl.2009.09.119

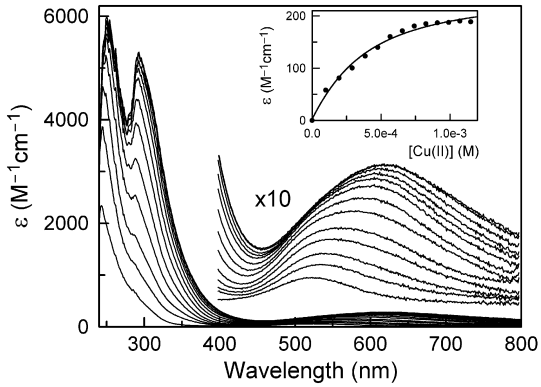


**Figure 1.** An optical titration of $Cu^{II}$ to Hn5 (200 μM) in 100 mM HEPES buffer at pH 7.0 (with 0.5-equiv increment from bottom to top).

assigned to $Cu^{II}$ in the HEXXH site and/or the di-His H7–H8 site as that in β-amyloid peptide (i.e., H13–H14).[20a] The detection of the two distinct d–d transitions suggests the presence of at least two specific $Cu^{II}$-binding sites in Hn5.

Electron paramagnetic resonance (EPR) spectroscopy is a very useful tool for the detection of compounds and materials with unpaired electrons, such as $Cu^{II}$ centers.[21] The EPR spectrum[22] of the 1:1 $Cu^{II}$–Hn5 complex (Fig. 2A) is axial with $g_{\|} = 2.188$, $g_{\perp} = 2.053$, and $A_{\|} = 612$ MHz and clear superhyperfine coupling in the $g_{\perp}$ region best fitted to three N-14 nuclei ($I = 1$) with two $A_N = 39.5$ MHz and one $A_N = 36.4$ MHz (Fig. 2A′). The spectral features are in good agreement with those of the square planar $Cu^{II}$–ATCUN site of bovine serum albumin ($g_{\|} = 2.177$, $g_{\perp} = 2.055$, and $A_{\|} = 603$ MHz and N-14 superhyperfine couplings)[19] and consistent with the conclusion from the electronic spectra. The superhyperfine couplings are possibly attributed to the two deprotonated amide-N atoms, the $N_{\delta}$ atom of His-3 residue, and/or the amino terminus which interact with the magnetic $d_{x^2-y^2}$ orbital of the square planar $Cu^{II}$. Particularly, the above amide and His N atoms are expected to bind to $Cu^{II}$ better due to their higher Lewis basicity than the amino group and are expected to exhibit the three superhyperfine couplings with Cu(II).

The addition of 2-equiv $Cu^{II}$ to Hn5 affords a spectrum which contains a mixture of two $Cu^{II}$-binding sites (Fig. 2B). The difference spectrum with spectrum A subtracted out (Fig. 2C) is due to the second $Cu^{II}$-binding site, which can be fitted with $g_{\|} = 2.261$, $g_{\perp} = 2.056$, and $A_{\|} = 540$ MHz (Fig. 2C′). These values are consistent with those observed for $Cu^{II}$ centers with predominantly N-containing ligands,[23] such as the H7–H8 site. Addition of up to 4 equiv of $Cu^{II}$ to the peptide results in another spectrum which is revealed in the difference spectrum with spectrum B subtracted out (Fig. 2D). It can be simulated with $g_{\|} = 2.312$, $g_{\perp} = 2.078$, and $A_{\|} = 520$ MHz (Fig. 2D′), consistent with predominantly oxygen-containing ligands,[23] such as an open coordination sphere with only a small number of coordinated His side chains in the equatorial position(s) interacting with the magnetic $d_{x^2-y^2}$ orbital of $Cu^{II}$. Possible candidates are the presumed $Zn^{II}$ binding HEXXH, the di-His H18–H19, and a non-specific His binding.

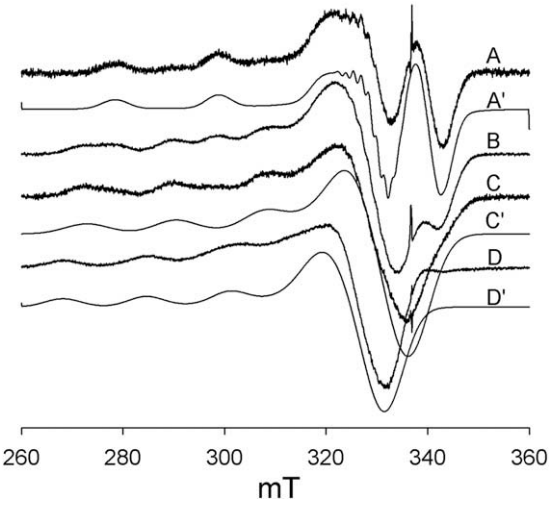


**Figure 2.** The EPR spectra of the $Cu^{II}$ complexes of Hn5 with different $Cu^{II}$:Hn5 ratios in DMF: (A) 1:1, with a small population of the second species in (B) subtracted out and (A′) is its fitted spectrum; (B) 2:1; (C) difference spectrum of (B–A) and the fitted spectrum (C′); and (D) 4:1, with the first two sites in B subtracted out and (D′) is the fitted spectrum.

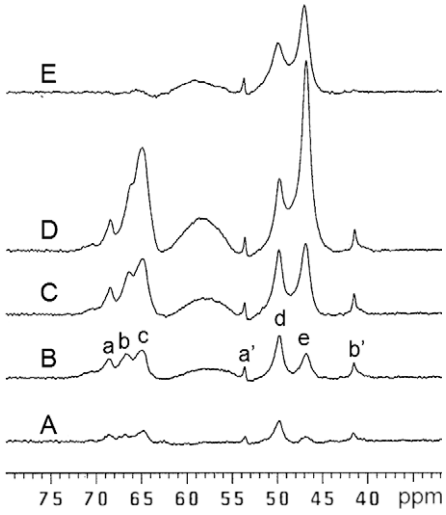


**Figure 3.** The $^1H$ NMR spectra of $Co^{II}$–Hn5 (2 mM) at (A) 0.5:1, (B) 1:1, (C) 2:1, and (D) 6:1 Co:Hn5 ratios in DMSO-$d_6$. (E) Addition of 5% $D_2O$ to (D) revealed five solvent exchangeable signals a–c, e, and b′.

Mononuclear $Cu^{II}$ centers can broaden the NMR signals of nearby protons beyond detection, rendering it difficult to study the complexes with NMR. Conversely, $Co^{II}$ has been utilized as a paramagnetic NMR probe for the study of the metal-coordination environment of various systems,[24] including serum albumin,[25] via the hyperfine-shifted signals. Upon addition of up to 1.0 equiv of $Co^{II}$ to Hn5 in DMSO, five hyperfine-shifted signals a–e (and two weaker signals a′ and b′) were detected[26] (Fig. 3A and B) in the typical range for the imidazole ring CH and/or NH protons of a $Co^{II}$-bound histidine residue.[24] Further addition of $Co^{II}$ increased the intensity of signals c and e (Fig. 3C and D). The spectral pattern indicates there are at least two $Co^{II}$ binding sites, signals a–d from one site and the overlapped c and e signals from the second site. The signals a–c (and b′) disappeared in the presence of 5% $D_2O$ while the signal e (overlapped) significantly decreases in intensity (Fig. 3E), indicating the presence of five (c is due to two overlapped signals) solvent exchangeable imidazole NH protons of $Co^{II}$-bound histidine residues.[24] Apparently, three of them (a, b, and c) are in the first $Co^{II}$-binding site which thus cannot be the N-terminus ATCUN site with only one His, while two (the overlapped c and e) are in the second site. Since there are two solvent non-exchangeable signals (d and the overlapped e), two of the coordinated His residue must adopt $N_{\delta}$-coordination mode; d in the first site and e in the second site. Such binding mode renders both $C_{\delta}H$ and $N_{\varepsilon}H$ protons farther away from the paramagnetic $Co^{II}$ center than the $C_{\varepsilon}H$ proton and show relatively sharper hyperfine-shifted $^1H$ NMR signals comparable to each other, of which $C_{\delta}H$ is not solvent exchangeable. In this case, the $C_{\varepsilon}H$ proton is *ortho* to $Co^{II}$, thus shows a much broader signal than the other two farther ring protons.

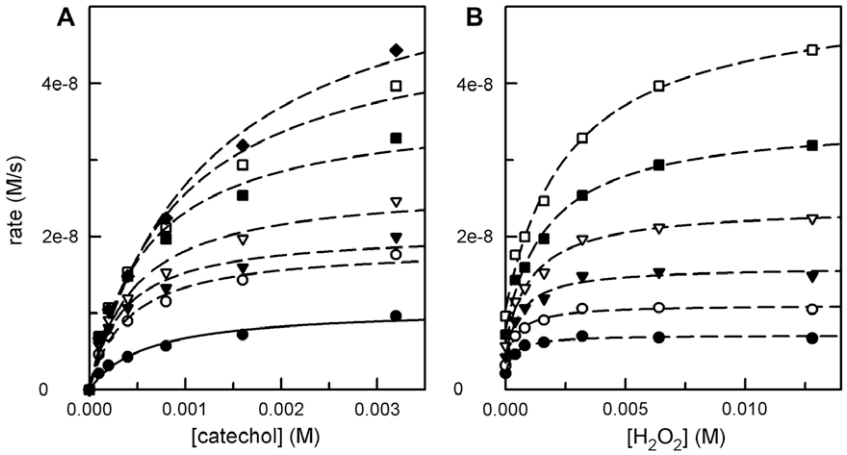


**Figure 4.** (A) Oxidation of catechol by 1.0 μM $Cu^{II}_2$–Hn5 in the presence of 0.0, 0.4, 0.8, 1.6, 3.2, 6.4, and 12.8 mM $H_2O_2$ (from bottom). (B) Oxidation of various amount of catechol (0.1, 0.2, 0.4, 0.8, 1.6, and 3.2 mM from bottom) by 1.0 μM $Cu^{II}_2$–Hn5 as a function of [$H_2O_2$]. Conditions: 100 mM HEPES buffer at pH 7.0 and 25 °C.

In a recent metal binding study of serum albumin,[25] $Co^{II}$ was found not to bind to the N-terminal ATCUN site. Owing to the similarity of the N-terminal metal-binding site between Hn5 and serum albumin (Fig. 3 and Ref. [19]), $Co^{II}$ probably also does not bind to the N-terminus of Hn5. In stead, $Co^{II}$ may bind to HEKHH or HH···H via two $N_\varepsilon$ and one $N_\delta$ atoms of His residues in the first site and two His residues via one $N_\varepsilon$ and one $N_\delta$ atom in the second site. The di-His metal-binding site in β-amyloid adopt $N_\varepsilon$ coordination mode,[20] which is likely to be the case for $Co^{II}$ binding in Hn5. The results thus suggest that $Co^{II}$ binds to Hn5 in an opposite order relative to $Cu^{II}$, wherein $Cu^{II}$ binds the N-terminus first whereas $Co^{II}$ does not seem to bind the N-terminus.

Since $Cu^{II}$ may be involved in the bioactivity of Hn[16] and is well known to exhibit redox chemistry by the use of $O_2$ or $H_2O_2$ as an oxidant, potential oxidative activity and mechanism of the $Cu^{II}_2$–Hn5 complex (with $Cu^{II}$ bound to the two sites in Fig. 2B) was investigated by the use of catechol (CA) as a substrate.[20,27] The rate of aerobic CA oxidation by $Cu^{II}_2$–Hn5 reaches a plateau at a high [CA] (●, Fig. 4A), indicating direct CA binding to the complex to form ($Cu^{II}_2$–Hn5)–CA intermediate, similar to the ES intermediate in enzymatic catalysis. Fitting the data to the Michaelis–Menten equation affords $k_{cat} = 0.011\ s^{-1}$ and $K_m = 0.59$ mM, which represents a $2.3 \times 10^4$-fold rate acceleration in terms of $k_{cat}/k_o$ with respect to the auto-oxidation rate constant[20b] $k_o = 4.74 \times 10^{-7}\ s^{-1}$.

The oxidation reagent $H_2O_2$ is a common ingredient in some hygienic products, including toothpaste. Thus, its influence on the oxidative activity of salivary $Cu^{II}_2$–Hn5 was investigated. The rate of aerobic CA oxidation by $Cu^{II}_2$–Hn5 increases with [$H_2O_2$], affording $k_{cat} = 0.060\ s^{-1}$, $K_m = 1.2$ mM, and $k_{cat}/K_m = 50\ M^{-1}\ s^{-1}$ at [$H_2O_2$] = 12.8 mM (♦, Fig. 4A), which is significantly higher than the rate without $H_2O_2$ (●, Fig. 4A). The rate of CA oxidative as a function of [$H_2O_2$] also follows the Michaelis–Menten kinetics at different [CA]'s (Fig. 4B), for example, $k_{cat}(H_2O_2) = 0.041\ s^{-1}$ and $K_m(H_2O_2) = 2.7$ mM at [CA] = 3.2 mM (□, Fig. 4B; affording a $4.7 \times 10^5$-fold rate acceleration relative to $k_o(H_2O_2) = 8.7 \times 10^{-8}\ s^{-1}$ determined for oxidation of 3.2 mM CA by $H_2O_2$). The kinetics indicates that $H_2O_2$ can bind to ($Cu_2$–Hn5)–CA to form a ternary $H_2O_2$–($Cu_2$–Hn5)–CA complex.

The catalytic mechanism may follow (a) a dinuclear or (b) a mononuclear pathway. The dinuclear pathway is analogous to that in catechol oxidase,[28] wherein the binding of CA to the di-$Cu^{II}$ center (which can be formed from the two bound $Cu^{II}$ ions or from two $Cu^{II}$ ions in different complexes) in the absence of $H_2O_2$ is followed by CA-to-$Cu^{II}_2$ two-electron transfer to afford the *o*-quinone product and a di-$Cu^{I}$ center. Oxygen then binds to the di-$Cu^{I}$ center, followed by two-electron transfer to produce a di-$Cu^{II}$–peroxo intermediate as found in catechol oxidase[28] and model complexes,[29] which further binds and oxidizes CA. In the presence of $H_2O_2$, the active di-$Cu^{II}$–peroxo intermediate is formed directly, followed by CA binding and oxidation.

In aerobic mononuclear pathway in the absence of $H_2O_2$, CA binding to $Cu^{II}$ is followed by CA-to-$Cu^{II}$ electron transfer to generate *o*-semiquinone–$Cu^{I}$ intermediate. Oxygen then binds to $Cu^{I}$, followed by two-electron transfer from the *o*-semiquinone–$Cu^{I}$ moiety to the bound $O_2$ to yield *o*-quinone product and a $Cu^{II}$–peroxo active intermediate which can bind and oxidize CA. In the presence of $H_2O_2$, the $Cu^{II}$–peroxo intermediate is formed directly which is followed by CA binding and oxidation. Several mononuclear $Cu^{II}$–peroxo complexes have been characterized[30] to support mononuclear Cu-centered oxidation reactions. The confirmation of the mechanism for the oxidative catalysis by Cu–Hn awaits further characterization of the $Cu_{(2)}$–peroxo intermediate.

Copper in the whole saliva can reach low-μM concentration.[31] Thus, it is essential to understand the interaction of $Cu^{II}$ with those salivary components capable of metal binding such as Hn5. The $Cu^{II}$–Hn5 complexes have been implied to play a vital role in the defense against microorganisms in the oral flora.[16] Herein, we conclude the presence of at least two specific $Cu^{II}$-binding sites in Hn5 and two sites (but excluding the ATCUN site) for $Co^{II}$ binding and that the $Cu^{II}_2$–Hn5 complex exhibits significant oxidative activity. The results suggest possible involvement of metal ions in the antimicrobial activity of Hn5 via metal binding and oxidative chemistry. Moreover, this peptide may serve as a template for the design of antibiotic metallopeptides against bacterial and fungal infections and metallopeptides for oxidative catalysis.

## Acknowledgments

The work on metallopeptide chemistry is supported by the National Science Foundation (L.-J.M.; CHE-0718625). This work was supported in part by the In-House Research Program of the National High Magnetic Field Laboratory (A.A.).

## References and notes

1. Oppenheim, F. G.; Xu, T.; McMillian, F. M.; Levitz, S. M.; Diamond, R. D.; Offner, G. D.; Troxler, R. F. *J. Biol. Chem.* **1988**, *263*, 7472.
2. MacKay, B. J.; Denepitiya, L.; Iacono, V. J.; Krost, S. B.; Pollock, J. J. *Infect. Immun.* **1984**, *44*, 695.
3. Murakami, Y.; Nagata, H.; Amano, A.; Takagaki, M.; Shizukuishi, S.; Tsunemitsu, A.; Aimoto, S. *Infect. Immun.* **1991**, *59*, 3284.
4. Tsai, H.; Bobek, L. A. *Antimicrob. Agents Chemother.* **1997**, *41*, 2224.

5. Tsai, H.; Bobek, L. A. *Biochim. Biophys. Acta* **1997**, *1336*, 367.
6. Pollock, J. J.; Denepitiya, L.; MacKay, B. J.; Iacono, V. J. *Infect. Immun.* **1984**, *44*, 702.
7. Paquette, D. W.; Waters, G. S.; Stefanidou, V. L.; Lawrence, H. P.; Friden, P. M.; O'Connor, S. M.; Sperati, J. D.; Oppenheim, F. G.; Hutchens, L. H.; Williams, R. C. *J. Clin. Periodontol.* **1997**, *24*, 216.
8. Oudhoff, M. J.; Bolscher, J. G. M.; Nazmi, K.; Kalay, H.; van't Hof, W.; Amerongen, A. V. N.; Veerman, E. C. I. *FASEB J.* **2008**, *22*, 3805.
9. Sabatini, L. M.; Ota, T.; Azen, E. A. *Mol. Biol. Evol.* **1993**, *10*, 497.
10. Vanderspek, J. C.; Wyandt, H. E.; Skare, J. C.; Milunsky, A.; Oppenheim, F. G.; Troxler, R. L. *Am. J. Hum. Genet.* **1989**, *45*, 381.
11. Raj, P. A.; Soni, S.-D.; Levine, M. J. *J. Biol. Chem.* **1994**, *269*, 9610.
12. Li, X. S.; Reddy, M. S.; Baev, D.; Edgerton, M. *J. Biol. Chem.* **2003**, *278*, 28553.
13. Baev, D.; Rivetta, A.; Vylkova, S.; Sun, J. N.; Zeng, G.-F.; Slayman, C. L.; Edgerton, M. *J. Biol. Chem.* **2004**, *279*, 55060.
14. Koshlukova, S. E.; Lloyd, T. L.; Araujo, M. W. B.; Edgerton, M. *J. Biol. Chem.* **1999**, *274*, 18872.
15. (a) Houghton, E. A.; Nicholas, K. M. J. *Biol. Inorg. Chem.* **2009**, *14*, 243; (b) Helmerhorst, E. J.; Troxler, R. F.; Oppenheim, F. G. *Proc. Natl. Acad. Sci. U.S.A.* **2001**, *98*, 14637; (c) Helmerhorst, E. J.; Breeuwer, P.; van't Hof, W.; Walgreen-Weterings, E.; Oomen, L. C. J. M.; Veerman, E. C. I.; Amerongen, A. V. N.; Abee, T. *J. Biol. Chem.* **1999**, *274*, 7286.
16. (a) Melino, S.; Gallo, M.; Trotta, E.; Mondello, F.; Paci, M.; Petruzzelli, R. *Biochemistry* **2006**, *45*, 15373; (b) Cabras, T.; Patamia, M.; Melino, S.; Inzitari, R.; Messana, I.; Castagnola, M.; Petruzzelli, R. *Biochem. Biophys. Res. Commun.* **2007**, *358*, 277.
17. (a) Melino, S.; Rufini, S.; Sette, M.; Morero, R.; Grottesi, A.; Paci, M.; Petruzzelli, R. *Biochemistry* **1999**, *38*, 9626; (b) Brewer, D.; Lajoie, G. *Rapid Commun. Mass Spectrom.*, 2000. 1736; (c) Grogan, J.; McKnight, C. J.; Troxler, R. F.; Oppenheim, F. G. *FEBS Lett.* **2001**, *491*, 76; (d) Gusman, H.; Lendenmann, U.; Grogan, J.; Troxler, R. F.; Oppenheim, F. G. *Biochim. Biophys. Acta* **2001**, *1545*, 86.
18. Peters, T., Jr. *Biochim. Biophys. Acta* **1960**, *39*, 546.
19. (a) Peters, T.; Blumenstock, F. A. *J. Biol. Chem.* **1967**, *242*, 1574; (b) Zhang, Y.; Wilcox, D. E. *J. Biol. Inorg. Chem.* **2002**, *7*, 327; (c) Harford, C.; Sarkar, B. *Acc. Chem. Res.* **1997**, *30*, 123.
20. (a) da Silva, G. F. Z.; Tay, W. M.; Ming, L.-J. *J. Biol. Chem.* **2005**, *280*, 16601; (b) da Silva, G. F. Z.; Ming, L.-J. *Angew. Chem., Int. Ed.* **2005**, *44*, 5501.
21. Palmer, G. In *Physical Methods in Bioinorganic Chemistry*; Que, L., Jr., Ed.; Spectroscopy and Magnetism; University Science Books: Sausalito, 2000 (Chapter 3).
22. EPR spectra were obtained on a Bruker Elexsys E580 cw/pulsed X-band spectrometer at ~5–6 K with a microwave frequency of 9.4 GHz at less than 2 mW, field modulation of 2 G or smaller for revealing superhyperfine coupling, and time constant of 40–80 ms. The spectra were fitted with EasySpin.
23. Peisach, J.; Blumberg, W. E. *Arch. Biochem. Biophys.* **1974**, *165*, 691.
24. (a) Bertini, I.; Luchinat, C.; Parigi, G. *Solution NMR of Paramagnetic Molecules*; Elsevier Science, B. V.: Amsterdam, The Netherlands, 2001; (b) Ming, L.-J. Nuclear Magnetic Resonance of Paramagnetic Metal Centers in Proteins and Synthetic Complexes. In *Physical Methods in Bioinorganic Chemistry: Spectroscopy and Magnetism*; Que, L., Jr., Ed.; University Science Books: Sausalito, 2000.
25. Mothes, E.; Faller, P. *Biochemistry* **2007**, *46*, 2267.
26. $^{1}$H NMR spectra were acquired on a Varian INOVA500 spectrometer (at 500 MHz $^{1}$H resonance) with a 5-mm bio-triple resonance probe. A 90° pulse (~6.0 μs) was used for the acquisition of the spectra with a presaturation pulse for solvent suppression. A line-broadening of 40 Hz was applied to improve the signal-to-noise ratio of the very broad hyperfine-shifted signals.
27. The initial rates of CA oxidation by $Cu^{II}$–Hn5 (with or without $H_2O_2$) were determined on a Varian Cary50 spectrophotometer, monitored at 500 nm by the use of 3-methyl-2-benzothiazolinone hydrazone (MBTH) as a trap for *o*-quinone to form a red adduct ($\varepsilon_{500} = 3.25 \times 10^4\ M^{-1}\ cm^{-1}$) (a) Espin, J. C.; Morales, M.; Varon, R.; Tudela, J.; Garcia-Canovas, F. *Anal. Biochem.* **1995**, *231*, 237; (b) Espin, J. C.; Tudela, J.; Garcia-Canovas, F. *Anal. Biochem.* **1998**, *259*, 118.
28. (a) Klabunde, T.; Eicken, C.; Sacchettini, J. C.; Krebs, B. *Natl. Struct. Biol.* **1998**, *5*, 1084; (b) Eicken, C.; Krebs, B.; Sacchettini, J. C. *Curr. Opin. Struct. Biol.* **1999**, *9*, 677.
29. Koval, I. A.; Gamez, P.; Belle, C.; Selmeczi, K.; Reedijk, J. *Chem. Soc. Rev.* **2006**, *35*, 814.
30. Itoh, S. *Curr. Opin. Chem. Biol.* **2006**, *10*, 115–122.
31. (a) Bales, C. W.; Freeland-Graves, J. H.; Askey, S.; Behmardi, F.; Pobocik, R. S.; Fickel, J. J.; Greenlee, P. *Am. J. Clin. Nutr.* **1990**, *51*, 462; (b) Chicharro, J. L.; Serrano, V.; Ureña, R.; Gutierrez, A. M.; Carvajal, A.; Fernández-Hernando, P.; Lucia, A. *Br. J. Sports Med.* **1999**, *33*, 204.